

Kinetics of Si monomer trapping at steps and islands on Si(001)

B. S. Swartzentruber

Surface and Interface Science, Sandia National Laboratories, Albuquerque, New Mexico 87185-1413

(Received 27 September 1996)

Si monomers are observed in empty-state scanning tunneling microscopy images acquired between room temperature and 115 °C. The monomers are trapped at the ends of rebonded *SB*-type dimer rows. When monomers thermally escape from the traps, they rapidly diffuse along the substrate dimer row until they find another unoccupied trap or return to their original trap. The binding activation barrier at isolated traps is ~ 1.0 eV. A slightly lower barrier exists for monomers to hop between the ends of neighboring dimer rows—a process facilitating diffusion along segments of *SB*-type steps. [S0163-1829(97)01803-1]

The growth of epitaxial thin films and overlayers occurs through the incorporation of deposited atoms into substrate crystal-lattice positions either at steps or islands. The details of the growth morphology depend on the interplay between a number of surface kinetic processes that determine the rate at which atoms ultimately become incorporated into the lattice. These processes are governed by the thermodynamic stability, or binding free energy, of various configurations, and may include atom or cluster diffusion, the formation and dissolution of islands, as well as attractive and repulsive interactions of atoms with various defects, including steps, islands, and other atoms. Of fundamental importance are the kinetics of monomers, namely, the sticking and residence times of monomers at steps and islands. In this work, the atomic-scale behavior of the binding of silicon monomers at steps and islands on the Si(001) surface is measured directly using variable-temperature scanning tunneling microscopy (STM).

The Si(001) surface reconstructs to form rows of dimerized atoms. Due to the crystal-lattice structure, the bond direction on alternating layers is orthogonal, which leads to two generally different types of steps. The edges of overlayer islands terminate with monatomic-height steps. As shown schematically in Fig. 1, step segments that are perpendicular to the lower-terrace dimer rows are called *SA* and those that are parallel to the lower-terrace dimer rows are called *SB*.¹ Furthermore, the *SB* steps can terminate in one of two locations with respect to the substrate dimer rows, ending either

at the trough between the dimer rows (so-called nonbonded *SB*) or on top of the dimer rows (so-called rebonded *SB*). In the latter case, the edge atoms of the step rebond with those in the last row of the lower terrace. The rebonded dimer bonds are depicted as gray in Fig. 1. The rebonded step configuration is energetically favored over the nonbonded step configuration.¹

Previous experimental work, pioneered by Mo and co-workers,²⁻⁵ used indirect methods to extract some kinetic parameters of Si monomer diffusion. Room-temperature STM measurements of island shapes and distributions quenched during homoepitaxial growth on Si(001) were compared with Monte Carlo simulations to estimate values for the anisotropic diffusion of Si monomers and the anisotropic sticking of monomers at the *SA* and *SB* steps.²⁻⁵ Recent low-temperature STM measurements on substrates cold enough to freeze out monomer diffusion have observed the stable monomer adsorption site on the terrace.^{6,7} The first theoretical study to accurately predict the stable monomer-terrace adsorption site was performed by Brocks, Kelly, and Car using first-principles methods.⁸ Several theoretical investigations have studied the interaction of monomers with steps using both first-principles⁹⁻¹¹ and empirical-potential¹²⁻¹⁴ methods. All of these calculations find that monomers are effectively noninteracting with *SA* steps but bind to *SB* steps in agreement with the experimental results of Mo and co-workers. However, the *ab initio* results predict that the monomers bind very strongly to the rebonded *SB* steps while they do not interact with the nonbonded *SB* steps. In direct contrast, results using empirical potentials predict that monomers bind to the nonbonded *SB* steps and are not interacting with the rebonded *SB* steps. As shown below, this dramatic contradiction is resolved through direct observation of the preferred monomer binding sites at steps. In addition, the monomer-step binding energy is obtained from measurements of the monomer dynamics performed at elevated temperature.

The experiments are performed in an ultrahigh vacuum chamber with a base pressure of 8×10^{-11} torr that contains the STM and an evaporative silicon source. The samples are cleaned by annealing to 1250 °C for several seconds.¹⁵ To evaporate silicon atoms onto the clean substrate surface a nearby silicon wafer is heated to ~ 1150 °C and an intervening shutter is opened for 10 s, resulting in the deposition of

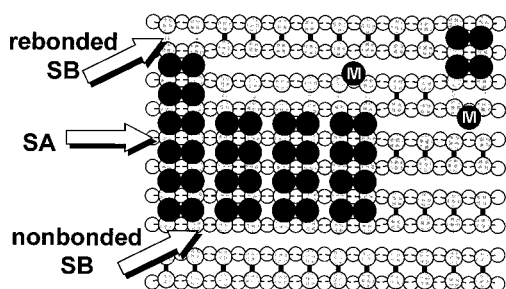


FIG. 1. Schematic of Si(001) surface showing various step terminations. Normal (rebonded) substrate dimer bonds are shown in black (gray). Two monomers *M* are depicted bound to traps sites at rebonded positions.

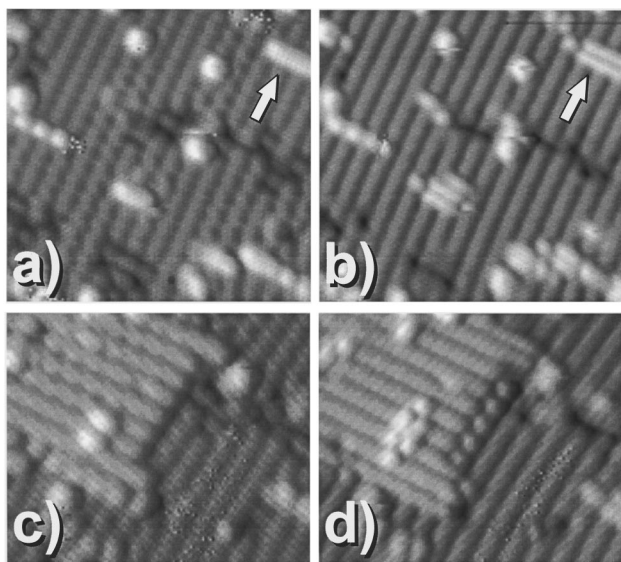


FIG. 2. Filled- (a), (c) and empty- (b), (d) state images of submonolayer Si growth on Si(001). Each pair of images, (a)-(b) and (c)-(d), was acquired simultaneously at room temperature. A single-dimer-wide island is indicated by the arrows.

several percent of a monolayer of silicon atoms. The substrate temperature during evaporation is $\sim 100^\circ\text{C}$. The samples are then transferred *in situ* to the variable-temperature STM where the temperature is set by resistive heating.^{16,17}

The contrast obtained in STM images of semiconductor surfaces is typically highly bias dependent, where the surface electronic-structure contrast may dominate over topographic contrast, i.e., which would be expected from the atomic coordinates.¹⁸ This is most evident in the comparison of images acquired using filled (occupied) and empty (unoccupied) states. Figure 2 shows filled- and empty-state images of two regions of the Si(001) surface after the deposition of several percent of a monolayer of silicon. The pairs of images were acquired simultaneously at room temperature—the filled states, (a) and (c), while scanning left to right and the empty states, (b) and (d), while scanning right to left.

Differences in the spatial contrast between the two images are clearly evident. One of the most notable is the apparent contrast on the substrate dimer rows which appear as stripes in the images. In the filled-state images, Figs. 2(a) and 2(c), the bright stripes on the substrate correspond to the tops of the dimer rows, whereas, in the empty-state images, Figs. 2(b) and 2(d), the bright stripes correspond to the regions between the dimer rows.¹⁹ Because the empty-state contrast is more sensitive to the dangling bonds, it is also much easier to see the structure associated with the individual atoms comprising clusters in the empty-state images. A short one-dimer-wide island appears as two narrow bands in the empty-state image and as one thicker stripe in the filled-state image [seen, for example, in the upper right corner of Figs. 2(a) and 2(b)]. However, within the scope of this work, the most important distinction between the filled- and empty-state images is that unpaired monomers at island and step

edges can be clearly imaged using empty states and are practically invisible using filled states. This is dramatically illustrated in the empty-state image of Fig. 2(d) in which monomers can be observed at the step edge. Historically, virtually all of the STM work on this surface measuring step and growth morphologies was performed using filled-state imaging, for the contrast in these images is more intuitively associated with the atomic structure. This may explain why information regarding the configuration and kinetics of monomer-containing structures has been lacking despite the vast amount of work on this system. The structural information contained in the empty-state images is now only beginning to be exploited both experimentally^{20,21} and theoretically.²²

When imaged at room temperature or above, after deposition at 100°C , unpaired monomers are found predominantly in one type of location that acts as a trap site. The monomers are bound only to the ends of *SB*-type dimer rows that have the rebonded termination. This observation directly confirms the predictions of the *ab initio* calculations^{9–11} and contradicts those expected from the empirical-potential methods.^{12–14} In this study, a monomer isolated on a terrace away from steps, islands, or clusters has never been observed. During the deposition process each monomer is able to find a stable binding site and/or the diffusion of an isolated monomer, even at room temperature, is so fast that it cannot be stably imaged and therefore remains unnoticed.

As easily determined from the images, trapped monomers are bound along the line of symmetry through the middle of the overlayer island dimer row; however, because of the strong electronic structure contribution to the image contrast, the exact position of the monomer along this line cannot be rigorously determined from the STM images. The *ab initio* calculations find the stable binding site at the so-called *M* position.^{10,11} The two monomers shown in Fig. 1 are bound to the ends of rebonded dimer rows at this position. Incidentally, monomers can also bind to the ends of the metastable diluted-dimer row structures;^{20,22} however, due to space limitations, these structures will not be discussed here.

The monomers can escape from their traps at elevated temperature. Once a monomer escapes, it very rapidly diffuses in a random walk along the substrate dimer row to which it was originally bound until it finds another unoccupied trap terminating on that row or it returns to the initial trap. The two monomers depicted in Fig. 1 are shown in trap sites terminating on the same dimer row. Certain defects in the substrate row and *SA*-type steps terminating across the row act as reflection barriers that effectively confine the monomers to one-dimensional segments of the surface. Because the rate of monomer diffusion is extremely high compared to the rate at which the monomers escape from the traps, the monomers are only imaged in the trap sites. In fact, in the STM images, the only monomers that are *observed* to vacate the trap sites are those that can exchange between two or more trap sites along a single substrate row. The monomers that have only a single trap accessible to them are always observed at the trap because upon leaving the trap they return on a time scale much more rapid than the imaging time scale.

Figure 3 shows monomers exchanging between trap sites in two pairs of sequential empty-state images acquired at

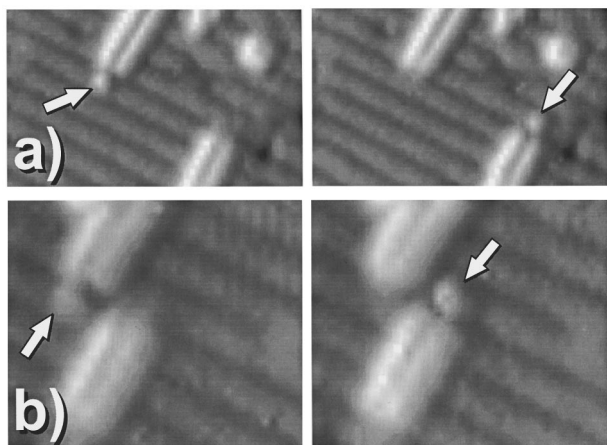


FIG. 3. Empty-state images of two pairs of monomer traps between which a monomer switches back and forth at 105 °C. The traps are separated by 11 and 3 lattice sites in (a) and (b), respectively. Location of monomer indicated by arrows. These movie images can be viewed on the World Wide Web at http://www.sandia.gov/surface_science/stm

105 °C. The two pairs of traps are separated by 11 and 3 lattice sites in Figs. 3(a) and 3(b), respectively. Each trap is a rebonded *SB*-type end of an island dimer row. Every pair of traps terminates on a single substrate dimer row, the top of which shows up as a dark band in these empty-state images. The fact that the monomers are stable in these configurations of traps for many minutes is testament to the enormous diffusional anisotropy of silicon monomers on the Si(001) surface, for if the monomers make even one hop across the channel to a neighboring row they are lost to the local system. Additional evidence for the difficulty of a cross-channel hop is indicated by the fact that two traps terminating on neighboring substrate dimer rows have never been observed to share a monomer. Therefore, even the local strain associated with the step rebonding does not induce the monomer to cross the channel. However, the monomers can freely cross over the top of the dimer row and bind to traps on the opposite side, as seen in Fig. 3. Pairs of traps in which a monomer binds on opposite sides of the substrate dimer row and those in which a monomer binds on the same side of the row exist with equal likelihood.

The rate at which a monomer escapes from a trap is determined by the binding activation barrier. The STM data show the number of times that a monomer is observed to switch traps during the acquisition of a series of images. The number of observed switches is a measure of the number of times that a monomer leaves one trap and successfully random walks to the other without returning to the initial trap. From the average residence time of the monomers in the trap sites at 105 °C, and assuming an attempt frequency of between 10^{12} and 10^{13} Hz,²³ the estimated binding activation barrier of the traps is $\sim 1.0 \pm 0.1$ eV.

There is a significant systematic difference between the rate that monomers escape from isolated traps, i.e., traps located at least several lattice sites from other islands or steps, and the rate that monomers switch between nearest-neighbor trap sites. In the process of switching between nearest-

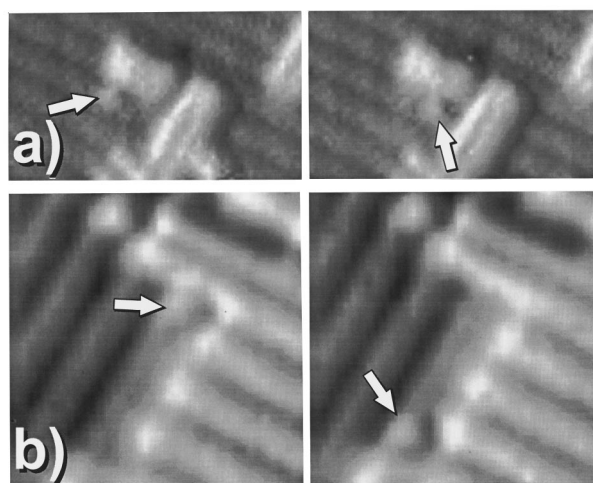


FIG. 4. A monomer (indicated by arrows) and nearest-neighbor traps at 105 °C. (a) Two traps comprised of short segments of neighboring-dimer rows in an island. (b) Section of *SB* step comprising a set of four aligned traps.

neighbor trap sites the monomer interacts only with rebonded-type substrate dimers—the gray dimer bonds in Fig. 1. Figure 4(a) shows two images of a pair of traps that are comprised of nearest-neighbor dimer rows. Here, two images are selected that show the monomer mostly in the trap site at the end of each dimer row. The residence times at such nearest-neighbor traps are systematically at least an order of magnitude shorter than at isolated traps, indicating a lower barrier for trap binding of at least 100 meV. Although some nearest-neighbor trap sites are found at islands, they appear commonly as straight segments of the *SB*-type steps. Figure 4(b) shows such a step configuration in which the ends of four neighboring dimer rows terminate on the same lower-terrace dimer row. Recall that dimer rows appear as dark stripes in the empty-state images. These four trap sites share a single monomer that is shown located at the two end sites in the two images. Again, monomers in this type of configuration switch sites significantly faster than those located at isolated traps. The barrier lowering at straight segments of the *SB* steps facilitates edge diffusion along the step, which in turn increases the rate that monomers find each other at the step during growth.

The large density of reactive trap sites at the steps implies that during growth, and at temperatures where thermal fluctuations occur, the relative occupation of monomers at the steps is rather high. Learning about the kinetics of monomer adsorption at steps is an important first step in understanding the propagation of the crystal lattice during growth. Future work will elucidate the additional details of the formation of the stable four-atom units demanded by the surface reconstruction, i.e., the formation and lifetime of metastable dimers and their subsequent capture of an additional two atoms.

In summary, active sites are found on the Si(001) surface that trap and bind Si monomers. These sites are located at the ends of rebonded *SB*-type dimer rows while nonbonded *SB* and *SA* steps are inert. At elevated temperatures, the binding activation barrier is estimated from the rate that monomers

switch between pairs of sites located on a single substrate dimer row. The binding activation barrier is somewhat lower at traps that are nearest neighbors to other traps, such as at straight segments of *SB* steps. The measurement of the kinetics of monomers yields much needed insight into the atomic-scale processes involved in the growth and thermal evolution of the surface. Additionally, observations of the relative stability and energetics of various atomic configura-

tions are necessary to enable the comparison and potential refinement of theoretical calculations.

I am grateful for many useful discussions with G. L. Kellogg, J. E. Houston, R. Stumpf, and P. J. Feibelman. This work performed at Sandia National Laboratories was supported by the U.S. Department of Energy under Contract No. DE-AC04-94AL85000.

-
- ¹J. D. Chadi, Phys. Rev. Lett. **59**, 1691 (1987).
²Y. W. Mo and M. G. Lagally, Surf. Sci. **248**, 313 (1991).
³Y. W. Mo, J. Kleiner, M. B. Webb, and M. G. Lagally, Phys. Rev. Lett. **66**, 1998 (1991).
⁴Y. W. Mo, Ph.D. thesis, University of Wisconsin-Madison, 1991.
⁵Y. W. Mo, J. Kleiner, M. B. Webb, and M. G. Lagally, Surf. Sci. **268**, 275 (1992).
⁶R. A. Wolkow, Phys. Rev. Lett. **74**, 4448 (1995).
⁷F. Wu, Ph.D. thesis, University of Wisconsin-Madison, 1996.
⁸G. Brocks, P. J. Kelly, and R. Car, Phys. Rev. Lett. **66**, 1729 (1991).
⁹Jun Wang, D. A. Drabold, and A. Rockett, Appl. Phys. Lett. **66**, 1954 (1995).
¹⁰Jun Wang, D. A. Drabold, and A. Rockett, Surf. Sci. **344**, 251 (1995).
¹¹Q.-M. Zhang, C. Roland, P. Boguslawski, and J. Bernholc, Phys. Rev. Lett. **75**, 101 (1995).
¹²C. Roland and G. H. Gilmer, Phys. Rev. Lett. **67**, 3188 (1991); Phys. Rev. B **46**, 13 437 (1992).
¹³Z. Y. Zhang, Y. T. Lu, and H. Metiu, Phys. Rev. B **46**, 1917 (1992).
¹⁴D. Srivastava and B. J. Garrison, Phys. Rev. B **47**, 4464 (1993).
¹⁵B. S. Swartzentruber, Y. W. Mo, M. B. Webb, and M. G. Lagally, J. Vac. Sci. Technol. A **8**, 210 (1990).
¹⁶N. Kitamura, B. S. Swartzentruber, M. G. Lagally, and M. G. Webb, Phys. Rev. B **48**, 5704 (1993).
¹⁷B. S. Swartzentruber and M. Schacht, Surf. Sci. **322**, 83 (1995).
¹⁸See, for example, *Scanning Tunneling Microscopy*, edited by J. A. Stroscio and W. J. Kaiser (Academic, New York, 1993).
¹⁹R. J. Hamers, R. M. Tromp, and J. E. Demuth, Surf. Sci. **181**, 346 (1987).
²⁰P. J. Bedrossian, Phys. Rev. Lett. **74**, 3648 (1995).
²¹B. S. Swartzentruber, A. P. Smith, and H. Jónsson, Phys. Rev. Lett. **77**, 2518 (1996).
²²G. Brocks and P. J. Kelly, Phys. Rev. Lett. **76**, 2362 (1996).
²³B. S. Swartzentruber, Phys. Rev. Lett. **76**, 459 (1996).